An Apparatus for Characterization and Control of Isolated Muscle

Waleed Farahat and Hugh Herr

Abstract—**An apparatus for characterization and control of muscle tissue is presented. The apparatus is capable of providing generalized mechanical boundary conditions to muscle tissue, as well as implementing real-time feedback control via electrical stimulation. The system is intended to serve as an experimental platform for implementing a wide variety of muscle control and identification studies that will serve as fundamental investigations of muscle mechanics, energetics, functional electrical stimulation, and fatigue. In one illustration of the capabilities of the apparatus, pilot experimental results of muscle workloops against a finite-admittance passive load are presented, illustrating how richer boundary conditions may reveal interesting muscle behavior.**

Index Terms—**Functional electrical stimulation (FES), mechanical boundary conditions, muscle characterization, muscle control, workloops.**

I. Introduction

MUSCLE biomechanists have evaluated the mechanical response of muscle cells and tissues using a variety of experimental approaches, including isometric force-length characterizations [1]–[5], force-velocity testing [6]–[9], quick release motion profiles [3], [4], and workloop testing [10]–[14]. These classical experimental protocols can be classified in one of two categories: 1) position-trajectory controlled experiments or 2) force-controlled experiments. In position-trajectory controlled experiments, the motion of the endpoints of the muscle-tendon structure is controlled as a predetermined function of time. This motion is usually delivered by means of a mechanical servo-system attached to the end points of the muscle-tendon structure. Consequently, the contractile forces generated by the muscle do not affect its endpoint motion trajectory. In distinction, in force-controlled experiments, the force imposed on the muscle is regulated independent of its motion. Therefore, as the muscle moves, there is no change in the reaction forces from its surroundings. Force controlled experiments are mostly implemented via a force feedback servo, but simple dead weights may be used. Examples of position-trajectory controlled experiments include isometric force-length experiments where muscle position is regulated at constant length, standard sinusoidal workloop experiments where muscle strain follows a sinusoidal path in time, and force-velocity experiments where the velocity is the independent variable. Examples of force-controlled experiments include quick release experiments, where the force imposed on the muscle is regulated to zero, and force-velocity experiments, where the force is the independent variable.

These two experimental categories offer two extremes of the load admittance range. In position-trajectory control mode, the admittance of the mechanical boundary conditions acting on the muscle is ideally zero (practically to within limitations of the servo-system used). In force-control mode, the admittance is ideally infinite, since there will be no change in force applied on the muscle due to a change in its length or velocity. Catering to such experimental requirements, standard off-the-shelf muscle testing systems provide dual-mode servo functionality, corresponding to these two extremes [15].

Therefore, the question arises as to whether testing for finite (but nonzero) admittance boundary conditions is necessary to fully characterize muscle tissue. Clearly, to understand *in vivo* tissue performance, muscle dynamics and the dynamics of the load on which the muscle acts upon must be taken into consideration. Examples of finite-admittance boundary conditions include loads such as springs, dampers, masses, drag friction, coulomb friction, or a combination thereof. Such loads prescribe boundary conditions that are generally defined in terms of dynamic relationships between force and displacement. Under these loading conditions, it would be expected that the dynamics of the load will interact with the contraction dynamics of the muscle, leading to a behavior that is a resultant of both. This is primarily because the force generated by the muscle is dependent on its mechanical state, namely its length and velocity. Several researchers characterized muscle under such loads by developing task specific apparatuses. Bawa [16], [17] characterized muscle under inertial and elastic loads. Krylow and Rymer [18] and Zhou [19] characterized muscle under pure inertial loading.

Aside from the need for generalized boundary conditions, there is increasing experimental interest in real-time control of muscle, primarily in the context of functional electrical stimulation (FES) [20]–[27]. In these investigations, attempts were made to control the response of muscle(s) and associated loads to a desired trajectory by varying electrical stimulation parameters as a function of time. Electrical stimulation patterns are typically square pulses characterized by frequency, amplitude, pulse-width and number of pulses per trigger (considering the cases of doublets, triplets, or more generally N-lets). In feedback experiments, these parameters are varied by a control algorithm to achieve a desired muscle response. Feedback con-

Manuscript received July 9, 2004; revised May 9, 2005; accepted July 27, 2005. This work was supported by the Defense Advanced Research Projects Agency (DARPA) under Award N66001-02-C-8034.

W. Farahat is with the Mechanical Engineering Department and The Media Laboratory, Massachusetts Institute of Technology, Cambridge, MA 02139 USA (e-mail: wfarahat@mit.edu).

H. Herr is with the Media Laboratory, Harvard–MIT Health Science and Technology Division, Massachusetts Institute of Technology, Cambridge, MA 02139 USA, and with the Department of Physical Medicine and Rehabilitation, Harvard Medical School, Spaulding Rehabilitation Hospital, Boston, MA 02114 USA (e-mail: hherr@media.mit.edu).

Digital Object Identifier 10.1109/TNSRE.2005.857686

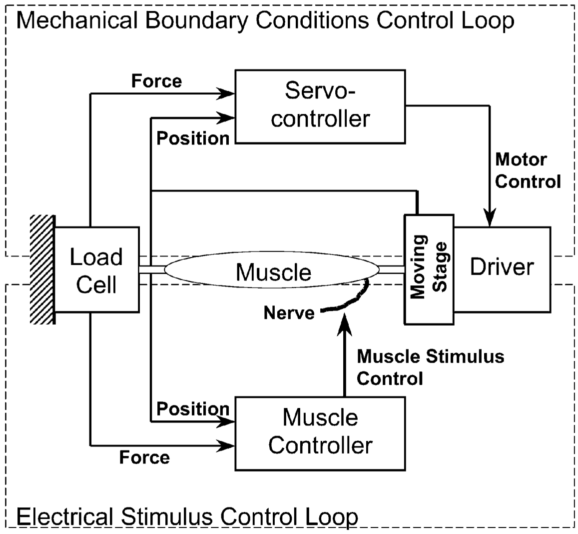

Fig. 1. Two control loops are operating simultaneously. MBC control loop causes the moving stage to simulate desired boundary conditions based on current position and force signals. ES control loop regulates muscle stimulus based on mechanical response.

trol via pulsewidth modulation has been popular [20]–[22], [24], [25] due to ease of implementation, and is preferred over amplitude modulation since it minimizes tissue damage [27]. In [26], frequency was modulated, and in [27], both frequency and pulsewidth were modulated. In [28] and [29], the number of pulses per cycle was modulated. For testing a variety of FES algorithms, an experimental apparatus is needed that is capable of real-time modulation of stimulation parameters as a function of a muscle's mechanical response.

In this paper, we present a system that can implement muscle testing protocols under generalized boundary conditions while also providing flexible feedback control of electrical stimulation parameters (see, for examples, [30]–[32]). These features are accomplished by having two real-time control loops running in parallel (see Fig. 1). The first loop, the mechanical boundary conditions (MBC) control loop, ensures that the mechanical response of the servo simulates the dynamics of the associated muscle boundary condition. For example, if the desired boundary condition is a linear spring, the MBC control loop controls the motion of the end points of the muscle-tendon to be proportional to the force generated by the muscle. The second loop implements the electrical stimulus control based on measurements of the muscle's mechanical response. This loop, referred to as the electrical stimulus (ES) control loop, offers simultaneous real-time modulation of pulse-width, amplitude, frequency, and the number of pulses per cycle.

In one experimental embodiment, dynamic boundary conditions may be applied to a muscle performing workloops. As a demonstration of the capabilities of the system, we present this new approach to workloop experiments for oscillatory power output measurements. The experiments were performed on *Plantarus longus* muscles of *Rana pipiens*. We show pilot data illustrating the difference between the finite-admittance testing method and current standard methods reported in the muscle workloops literature [10].

In Section II, we provide a description of the apparatus, and in Section III, we discuss various experimental protocols that are easily implemented using the apparatus. Finally, in Section IV, we present workloop experimental data of muscle acting against finite and zero-admittance boundary conditions.

II. Muscle Testing Apparatus

Fig. 2 summarizes the system. A description of its functional requirements and components follows.

A. Functional Requirements

Off-the-shelf dual-mode servo muscle testing systems are capable of generating classical muscle characterizations mentioned in Section I. In addition, the following functional requirements are recognized:

1) Capability to Implement Generalized Dynamic Boundary Conditions on Muscle: This involves simulating the different mechanical environments with which a muscle interacts. A flexible approach would be to simulate such environments in software and allow for a servo-system to deliver their response. The servo-system needs to be responsive enough to accommodate force disturbances generated by the muscle. A bandwidth > 120 Hz was determined as a requirement for the muscles under consideration (*Rana pipien* jumping muscles). This estimate was based on the rise time of a typical twitch force profile (typically 40 ms). This requirement is fulfilled by the MBC control loop shown in Fig. 1. A closed-loop impedance of 20 kN/m, approximately corresponding to 1% muscle strain at maximum force, was deemed sufficient.

2) Electrical Stimulus Real-Time Feedback Control: For FES and control purposes, the system should allow for real-time changes to the signal parameters as a function of the muscle's mechanical state. This requirement is fulfilled by the ES control loop shown in Fig. 1.

3) Testing of Agonistic/Antagonistic Muscle Pairs: In a single muscle arrangement, the force and impedance of the muscle are both modulated simultaneously by its activation level. At least two muscles are needed to achieve independent control of impedance and net force generation over a joint. A testing apparatus, or a combination of apparatuses, should be capable of mimicking a situation where agonistic and antagonistic muscles act against a common load. This requirement is fulfilled by connecting two testing apparatuses to the same personal computer (PC), and controlling them by the same real-time process. The two systems are therefore linked in software, and are essentially seeing the same virtual load. As the antagonistic contracts, the agonist stretches commensurately. Under this arrangement, not only can the system be used for motion trajectory control via the muscle pair, but also for muscle impedance control strategies.

B. Sensors/Actuators

The sizing of the components for the apparatus depends on the type of muscles desired for experimentation. The particular unit presented here is sized to accommodate muscles extracted from *Rana pipien* frogs (e.g., *semitendinosus*, *semimembranosus*, *plantarus longus*, etc.). These muscles are typically

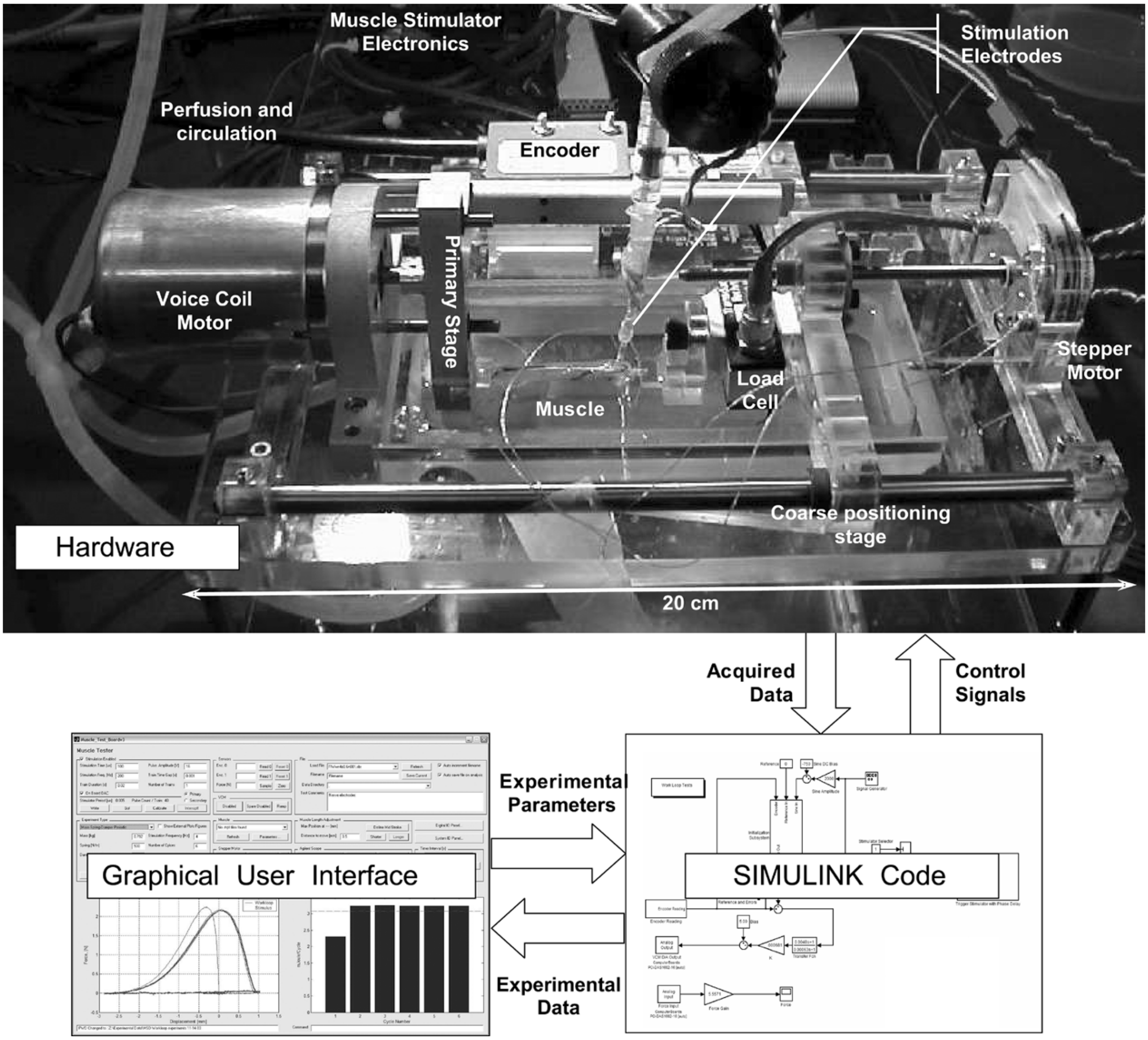

Fig. 2. Overall system summary. Experimental definitions and parameters are entered via the graphical user interface, which in turn invokes the appropriate SIMULINK block diagram and downloads the experimental parameters. The real-time code then takes control over the hardware to acquire the muscle data, which is then sent back to the GUI for postprocessing. Apparatus is shown above with the primary sensors and actuators noted. Coarse positioning stage is adjusted at the beginning of the experiment to accommodate different lengths, but is typically kept at a constant position during a particular contraction. Primary stage provides the motion that simulates the boundary conditions. Muscle shown in the apparatus is a frog (*Rana pipien*) *semimembranosus* muscle submerged in Ringer's solution. Vertical syringe has a suction electrode at its tip that is connected to the stimulation electronics in the background. Silicone tubing recirculates solution via a peristaltic pump, while oxygen is injected in the loop.

less than 15–25 mm in length (muscle belly, at l_o, the length corresponding to maximum force output), with a mass < 1 g. The maximum forces generated by these particular muscles are on the order of 3–5 N. *In vivo* aggregate strains are generally less than $\pm 15\%$, resulting in end point motion of less than ± 4 mm [33], [34]. The time to peak force in a twitch is typically 30–40 ms. During apparatus design, these figures guided the selection of sensors and actuators.

A two-actuator approach was used to achieve large-stroke and high-bandwidth.

1) A linear stepper motor actuator (Haydon Switch and Instruments, Waterbury, CT) provides a large travel stroke of the coarse positioning stage, covering a total span of over 100 mm. The actuator is driven by a bipolar stepper motor driver.
2) A high-bandwidth voice coil motor (VCM) (BEI Kimco, Vista, CA) provides fine positioning of the primary stage. A transconductance H-bridge amplifier (Centent Company, Santa Ana, CA) drives current through the VCM, resulting in a force proportional to current that acts on the moving mass. The VCM has a smaller stroke $(\pm 4 \text{ mm})$[1] and a stall force of $(\pm 30 \text{ N})$.

During initialization of a particular experiment, the coarse stage positioning stepper motor is adjusted to accommodate the nominal length of the muscle under experimentation. Its location is typically held fixed for the duration of the experiment.

[1]This stroke range is sufficient for *in vivo* like strains for the muscles considered. Larger strokes may be achieved by combined dual control of the linear stepper motor and the VCM [35]. While this feature has not been implemented yet, its implementation is straight-forward within the software framework described.

The high-bandwidth actuator takes control to provide desired endpoint motions, rejecting disturbances due to muscle contraction via the servo loop.

Position sensing is attained by a 1 μm resolution, incremental, noncontact magnetic encoder (SIKO Products, Dexter, MI). In-series force sensing is attained via a strain-gage-based load cell (Transducer Techniques Inc., Temecula, CA) in conjunction with a wheat-stone bridge amplifier.[2]

An electric stimulator with real-time programmable pulse parameters is implemented via an H-bridge design on a custom built breakout board. The stimulus is controlled by a field programmable gate array that controls all stimulus timing parameters. Stimulator specifications are provided in Table III.

C. Integration and Design

The sensors and actuators are mechanically integrated into the design shown in Fig. 2. A breakout board was designed to integrate all the system components electrically, to provide stimulation to the muscle via an onboard programmable stimulator, and to act as a communication interface between the hardware and the real-time software.

D. Mechanical Boundary Conditions Control Loop

As is the case with standard muscle testing apparatuses, the mechanical boundary conditions control loop can be operated in direct position-trajectory control mode and in force-control mode. Additionally, implementation of simulated dynamic boundary conditions is achieved by directly measuring the muscle force, filtering it through the transfer function of the desired boundary condition, and directing the result as the new reference position of the servo controller. This assumes that the bandwidth of the servo-system is high enough to accommodate the dynamics of the simulated boundaries, and that the backloading effects of the muscle are small. Typically, this condition is satisfied. Boundary conditions of interest have natural frequencies < 10 Hz, which is well below the servo-system bandwidth.

Experimentally identified closed-loop bode plots confirm a -3 dB bandwidth of 150 Hz for the MBC control loop (see Fig. 5). Root locus analysis was performed to ensure that this bandwidth and stability are not compromised as the muscle stiffness changes. Appendix I summarizes the system's servo-mechanical performance metrics.

E. Electrical Stimulus Control Loop

The electrical stimulus applied to the muscle is a pulse train that is characterized by amplitude, pulse width, period between pulses, and number of pulses per trigger. All four quantities can be controlled in real-time, simultaneously and independently. In feedback muscle control experiments, these parameters are typically a function of the mechanical response of the muscle-actuated system (that is, the muscle in a given experiment, and its virtual load that is simulated by the mechanical boundary conditions control loop). Table III summarizes the electrical stimulator specifications.

[2]The in-series measured force is assumed to be entirely due to the contraction of the muscle. Inertial effects due to acceleration of the muscle mass were estimated to be three orders of magnitude less than its contractile force, and therefore safely neglected.

F. Control Implementation

Real-time control, data acquisition and storage are implemented under the MATLAB Real-Time Workshop, Simulink and the xPC Target (Mathworks Inc., Natick, MA). A multipurpose data acquisition card (Measurement Computing) is used in conjunction with a target PC to communicate with the breakout board. Control and data acquisition sampling rates are set at 2 kHz. A library of block diagrams implementing different experimental logics is developed. New experiments are easily added since all that is required is the generation of the appropriate Simulink block diagram.

G. Graphical User Interface

A graphical user interface implemented in MATLAB's Graphical User Interface Development Environment Guide allows the user to select and control all experimental parameters. The interface invokes the real-time code to operate and trigger data-acquisition for a particular experiment. It also invokes appropriate subroutines for high-level data post-processing and plotting.

III. Experimental Applications

In this section, we provide descriptions of potential experimental protocols that can be implemented using the muscle testing apparatus.

A. Muscle Identification Experiments

Basic open-loop muscle identification experiments including force-length, force-velocity, quick release, and workloop characterizations can be implemented using the apparatus. Here, the term open-loop refers to the electrical stimulus since it is predetermined at the start of an experiment. In classical muscle characterization experiments, the boundary conditions implemented have generally been constant length, constant velocity or constant force boundary conditions [3], [4], [7]–[9]. Furthermore, pseudo-binary random sequence (PBRS) identification and deconvolution methods have been implemented under isometric conditions to identify the muscle recruitment characteristics [25], [30], [36]. The apparatus presented here may extend these experiments in the context of generalized boundary conditions.

B. Position/Force Control of a Simulated Load Using Electrical Stimulus Feedback

The objective of this experiment would be to test algorithms for position control of a known load via muscle actuation. See for example [30] and [32]. Here, the MBC control loop would simulate the dynamics of the load, (e.g., a second-order mass-spring-damper system) while the ES control loop would implement the algorithms being evaluated.

C. Impedance Control of Agonistic/Antagonistic Pairs

It is known that co-contraction is employed to increase the output impedance of muscle-actuated systems [37]. Implementing impedance control (without human supervisory

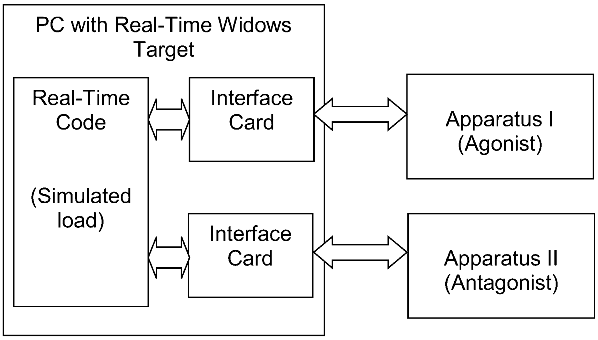

(a) System setup

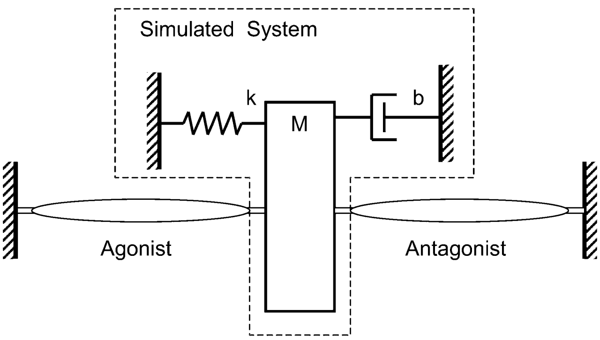

(b) Agonist-antagonist pair acting on common load

Fig. 3. (a) Setup for agonist antagonist control experiments. (b) Two testing apparatuses are controlled by the same program, simulating the physical system.

control as in [31]) in electrically stimulated muscle systems has not been demonstrated experimentally to the authors' knowledge, and is considered an open area of research. Using two apparatuses in an agonistic/antagonistic muscle testing arrangement (as shown in Fig. 3) would allow for the testing of control strategies with impedance as the desired output. Here, the impedance of the closed loop (muscle plus simulated load) system would be measured via perturbation response.

D. Fatigue Studies

It has been reported that the number of pulses per cycle affects the fatigue life of a muscle undergoing electrical stimulation [28], [29]. The experiments in [28] and [29] focused on isometric development. Using the apparatus presented, fatigue studies may be implemented under generalized boundary conditions.

E. Identification of Muscle Workloop Power Output Under Finite Admittance Boundary Conditions

The capacity of muscles to generate mechanical power output has been characterized in terms of workloops. In [10], Josephson presented a method of measuring muscle workloop output under sinusoidal conditions. This method set the standard for muscle workloop testing in the muscle physiology literature. Briefly described, the muscle is subjected to prescribed sinusoidal length variations in time. An electrical stimulus is triggered at a particular phase of the cycle, resulting in a contractile force. A plot of force versus displacement results in a workloop plot [as in Fig. 4(a) and (c)]. The area enclosed in the workloop is a measure of mechanical the work output by the muscle. In [10]–[12], [14], [38]–[41], the dependence of the energetics of muscles on electrical stimulus parameters was investigated, and was correlated with the biological functionality of particular muscles.

The testing methodology in [10] is essentially an zero-admittance testing methodology. A richer test would be to have the muscle perform workloop experiments under passive, finite-admittance loads. In this scheme, the muscle stimulus is triggered at a particular frequency. Consequently, a force is generated that results in a motion trajectory that is dependent on the boundary conditions. This alters the character of the workloop output of the muscle, and, therefore, the muscle energetics estimate. Sample results for this particular experiment are presented in Section IV.

IV. Pilot Data of Workloop Experiments

In this section, we present pilot data on the workloop experiments described in Section III-E. Pilot data are presented as an illustration of the system's capacity to measure workloop power production under finite-admittance boundary conditions. Using the MBC control loop, a second order mass-spring-damper system is simulated as the compliant boundary condition against which the experimental muscle specimen acts. This experiment is designed to show how muscle power output may change significantly in the context of a finite-admittance boundary condition compared to the traditional zero-admittance motion source first proposed by Josephson [10].

A. Methods

Plantarus longus muscles were dissected out of adult male *Rana pipiens* (approximately 30-g frogs). Prior to removal from the animal, the muscle rest length was measured with both the knee joint and the hip joint positioned at 90°. To minimize tendon damage, the muscle was removed with bone chips attached to both ends. A reflex clip was stapled to the bone chips, tightly sutured, and secured to the interface points in the testing apparatus via a dove tail connection (the muscle's distal end to the primary stage, and the proximal end to the coarse positioning stage through the load cell). Periodic testing throughout the experiment ensured that there was no slack or slippage of the muscle specimen. Tests included visual inspection, as well as monitoring the shape and peak levels of single isometric twitch force profiles. The muscle was submerged in a tub of Ringer's solution that was circulated via a peristaltic pump. The solution was generously oxygenated via direct O_2 gas bubbling at an insertion point in the circulation loop.

Stimulation was delivered through a suction electrode to the sciatic nerve of the muscle. Initial successive isometric twitch measurements were used to establish full recruitment voltage levels, beyond which there was no increase in force production. Additionally, isometric twitch tests were interleaved periodically within experimental measurements to ensure that the muscle did not fatigue, and that force production levels remained constant throughout the duration of the experimental session. When muscle twitch force levels decreased to below 90% of their initial value, the ensuing data were discarded.

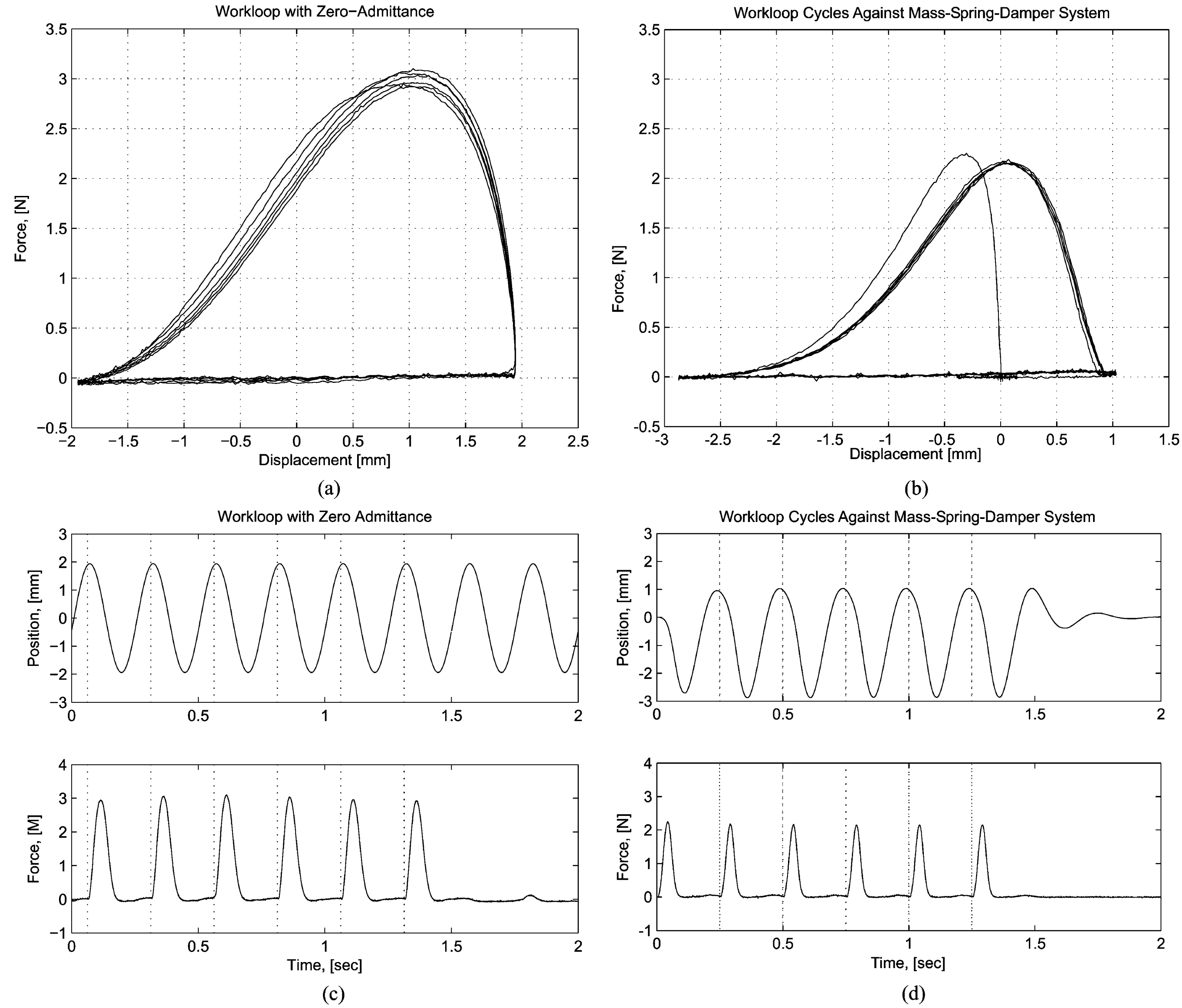

Fig. 4. Comparison of zero-admittance workloops (ZAW) versus finite-admittance workloops (FAW). Here, the FAW power output was 56% of that of the ZAW. (a) Sinusoidal stimulation with frequency of 4 Hz and amplitude $= 20\%$ strain. (b) Workloop plot with a mass-spring-damper boundary condition. Parameters for this particular measurement are: $m = 0.79$ kg, $k = 500$ N/m, $b = 11.9$ Ns/m. These parameters were chosen such that the natural frequency $\omega_n = 4$ Hz $=$ stimulation frequency, damping ratio $\zeta = 0.3$, and static gain $k_s = 10\%$ strain at maximum force generated. (a) Zero-admittance workshop. (b) Finite-impedance workloop. (c) Zero-admittance position and force time trajectories. (d) Finite-impedance position and force time trajectories.

Electrical stimulus parameters were set at pulse frequency $=$ 200 Hz, pulsewidth $=$ 100 μs, and amplitude $=$ full recruitment voltage.[3] Two sets of data with stimulation durations of 40 and 60 ms were acquired. For the zero-admittance cases, the stimulation was triggered at 90° phase, corresponding to the point of maximal stretch.

In the zero-admittance case, the motion of the endpoints was sinusoidal with a frequency of 4 Hz and an amplitude of ± 2 mm. Correspondingly, for the finite admittance case, the natural frequency of the passive load and the frequency of the stimulus trigger were both set at 4 Hz. The stimulus trigger was matched with the system's resonance frequency so as to produce maximum amplitude excursions. This condition provided the highest energy absorption in the simulated damper, or the highest muscle workloop power output. The static stiffness of the simulated load was set such that the resulting motion had the same amplitude as that of the zero-admittance case for relevant comparison.

B. Results

Sample experimental results are plotted in Fig. 4. In the zero-admittance case [Fig. 4(a) and (c)], the motion was driven by the servo-system, and the muscle force did not affect its motion trajectory. In the finite admittance case [Fig. 4(b) and (d)], the motion was caused by the muscle force.

Energy output was estimated by integrating the areas inside the workloops. To normalize the results, power output was

[3]In the muscle workloop literature (see for example [10], [11], and [33]), the muscle is typically overstimulated to guarantee full recruitment. While this decreases the *in vitro* life of the muscle, we opted to use such patterns to enable relevant comparison with established data.

TABLE I
EXPERIMENTAL WORKLOOP MUSCLE POWER OUTPUT

Stimulation Duration	FAW [Watt/kg]	ZAW [Watt/kg]	Ratio [%]
40 ms	14.7 ± 0.25	29.3 ± 0.43	50.1
60 ms	18.0 ± 0.38	31.7 ± 0.31	56.8

divided by the total muscle mass. The normalized results are summarized in Table I. Under the described conditions, muscle preparations typically lasted for 5–15 data sets (similar to that shown in Fig. 4) over the course of 1–3 h.

V. Discussion

The measurements of Section IV indicate that although the motion of the muscle had the same frequency and peak-to-peak amplitude in both the zero and finite admittance cases, the power output was substantially different (almost by a factor of 2). This is primarily attributed to the dependence of muscle force output on its mechanical state. Changing boundary conditions changes the dynamic relationship between state and force, and, therefore, the character of the work output.

While these experimental results are meant as an illustration of the capabilities of the testing apparatus, they lead to a set of interesting research directions regarding muscle energetics. Specifically, there is a need to understand how muscle workloop performance changes with boundary condition admittance, as described by natural frequency, damping ratio, and spring stiffness. Experiments of this nature may provide important insights as to how muscle power output is affected by the nature of the task at hand, and in light of variations in muscle environment. While it not surprising that the power generated by a muscle is influenced by its boundary conditions, the methods presented provide a direct means of quantification.

In the muscle control arena, the apparatus may also be employed to investigate the merits of different algorithms. Typical muscle control investigations, specially in the context of FES, are conducted on limbs where muscular contraction dynamics confound with complexities of skeletal dynamics. This results in a highly complicated problem. One way to decompose this complexity is to simulate idealized loads acted upon by the muscle. The apparatus presented here allows for the implementation of such idealized loads precisely via the MBC control loop. This includes linear, nonlinear, as well as loads that simulate actual *in vivo* biomechanics. The simulation of idealized loads in series with the muscle specimen allows the experimenter to focus only on the muscle control problem. Once adequate control schemes are advanced for these idealized boundary conditions, one may then move to more complex environmental muscle conditions.

The muscle testing system presented provides a versatile platform for generalized muscle testing experiments, in open-loop stimulation, as well as closed-loop stimulation modes. Additional system functionality may be added with minimal software development (primarily the development of the associated Simulink block and adding relevant GUI controls). The flexibility of the system stems from its capacity to implement simulated boundary conditions on the tested muscles, coupled with its capacity to modulate electrical stimulus parameters in real-time based on a computed control output. In future studies on muscle behavior, we anticipate this platform will support a wide variety of muscle control and identification investigations.

TABLE II
SERVO-MECHANICAL SPECIFICATIONS

Displacement	Total coarse positioning range	0 - 100 mm
	Sensing resolution	1 μm
	Voice coil motor range	8 mm
Force	Sensing range	± 22.5 N
	Sensing resolution	1 mN
Bandwidth	Open-loop	92 Hz
	Closed-loop	153 Hz
	Gain margin	14 dB
	Phase margin	> 50 degrees
Voice coil motor	Stall Force	± 30 N

TABLE III
STIMULATOR ELECTRICAL SPECIFICATIONS

Amplitude	Max	16.2 V
	Resolution	0.25 mV
	Saturation Current	25 mA
Output Impedance	Driving high	4.7 Ω
	Driving low	2.2 Ω
Waveform	Bipolar square pulses,	both electrodes driving
Pulse width	Max	0.32 s
	Resolution	1 μs
Pulse interval	Max	0.32 s
	Resolution	1 μs
Pulse count	1 to 65,536	pulses per trigger

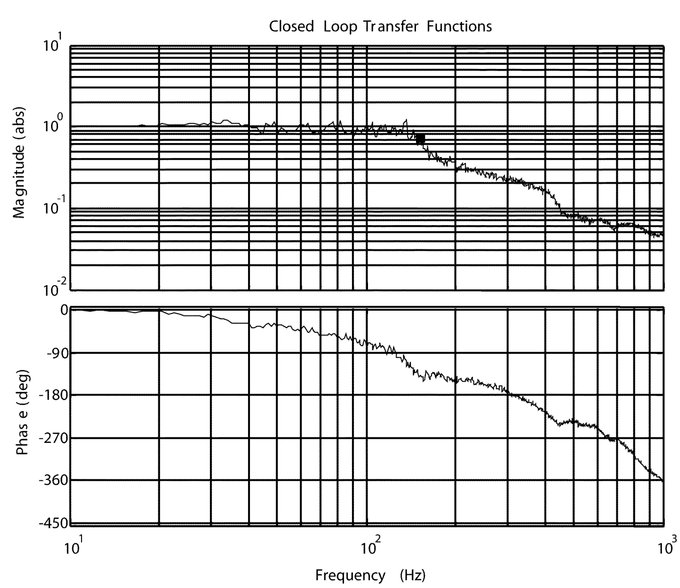

Fig. 5. Unloaded closed-loop position frequency response of the MBC control-loop. Shown is the experimentally measured transfer function from desired reference motion to actual motion. The -3 dB bandwidth was measured at 153 Hz. Actuator reference signal was white noise (to within sampling frequency), with a standard deviation $\sigma = 1$ mm, implying a 6σ range of ± 3 mm.

APPENDIX
SYSTEM SPECIFICATIONS

The performance specifications of the servo-mechanical system are summarized in Table II. Table III shows the specifications of the electrical stimulus parameters. Fig. 5 shows the closed-loop position frequency response of the MBC control-loop.

ACKNOWLEDGMENT

The authors would like to thank Dr. A. Ahn for her muscle preparations and advice in muscle experimentation. The authors also wish to thank C. Bolton for his implementation of the breakout board.

REFERENCES

[1] A. V. Hill, "The effects of series compliance on the tension developed in the muscle twitch," *Proc. R. Soc. London*, vol. 138, pp. 325–329, 1951.

[2] ——, "The series elastic component of muscle," *Proc. R. Soc. London*, vol. 137, pp. 237–280, 1950.

[3] R. C. Woledge, N. A. Curtin, and E. Homsher, *Energetic Aspects of Muscle Contraction*, ser. Monographs of the Physiological Society no. 1. San Diego, CA: Academic, 1985.

[4] T. A. McMahon, *Muscles, Reflexes and Locomotion*. Princeton, NJ: Princeton University Press, 1984.

[5] A. F. Huxely and R. M. Simmons, "Mechanical properties of the cross-bridges of frog striated muscle," *J. Physiol.*, vol. 218, pp. 59–60, Oct. 1971.

[6] A. V. Hill, "The heat of shortening and the dynamic constants of muscle," *Proc. R. Soc. London*, vol. 126, pp. 136–195, 1938.

[7] K. A. P. Edman, "The velocity of unloaded shortening and its relation to sarcomere length and isometric force in vertebrate muscle fibers," *J. Physiol.*, vol. 291, pp. 143–159, 1978.

[8] H. Mashima, "Force-velocity relation and contractility in striated muscles," *Jpn. J. Phys.*, vol. 34, pp. 1–17, 1984.

[9] A. S. Bahler, J. T. Fales, and K. L. Zieler, "The dynamic properties of mammalian skeletal muscle," *J. General. Physiol.*, vol. 51, pp. 369–384, 1968.

[10] R. Josephson, "Mechanical power output from striated muscle during cyclic contraction," *J. Exp. Biol.*, vol. 114, pp. 493–512, 1985.

[11] E. D. Stevens, "The pattern of stimulation influences the amount of oscillatory work done by frog muscle," *J. Physiol.*, vol. 494, no. 1, pp. 279–285, 1996.

[12] ——, "Effect of pH and stimulus phase on work done by isolated frog sartorius muscle during cyclical contraction," *J. Muscle Res. Cell Motility*, vol. 9, pp. 329–333, 1988.

[13] D. Stokes and R. Josephson, "The mechanical power output of a crab respiratory muscle," *J. Exp. Biol.*, vol. 140, pp. 287–299, 1988.

[14] R. Josephson and D. Stokes, "Strain, muscle length and work output in a crab muscle," *J. Exp. Biol.*, vol. 145, pp. 45–61, 1989.

[15] Aurora Scientific (2004). [Online]. Available: http://www.aurorascientific.com/

[16] P. Bawa, A. Mannard, and R. B. Stein, "Predictions and experimental tests of a visco-elastic muscle model using elastic and inertial loads," *Biol. Cybern.*, vol. 22, pp. 139–145, 1976.

[17] ——, "Effects of elastic loads on the contractions of cat muscles," *Biol. Cybern.*, vol. 22, pp. 129–137, 1976.

[18] A. Krylow and W. Z. Rymer, "Role of intrinsic muscle properties in producing smooth movements," *IEEE Trans. Biomed. Eng.*, vol. 44, no. 2, pp. 165–175, Feb. 1997.

[19] B.-H. Zhou, S. R. Katz, R. V. Baratta, M. Solomonow, and R. D. D'Ambrosia, "Evaluation of antagonist coactivation strategies elicited from electrically stimulated muscles under load-moving conditions," *IEEE Trans. Biomed. Eng.*, vol. 44, no. 7, pp. 620–633, Jul. 1997.

[20] H. J. Chizeck, P. E. Crago, and L. Kofman, "Robust closed loop control of isometric muscle force using pulsewidth modulation," *IEEE Trans. Biomed. Eng.*, vol. 35, no. 7, pp. 510–517, Jul. 1988.

[21] G. F. Wilhere, P. E. Crago, and H. J. Chizeck, "Design and evaluation of a digital closed loop controller for the regulation of muscle force by recruitment modulation," *IEEE Trans. Biomed. Eng.*, vol. 32, no. 11, pp. 668–676, Sep. 1985.

[22] P. H. Veltink, H. J. Chizeck, P. E. Crago, and A. El-Bialy, "Nonlinear joint angle control of artifically stimulated muscle," *IEEE Trans. Biomed. Eng.*, vol. 39, no. 4, pp. 368–380, Apr. 1992.

[23] J. Giuffrida and P. E. Crago, "Reciprocal EMG control of elbow extension by FES," *IEEE Trans. Neural Syst. Rehabil. Eng.*, vol. 9, no. 4, pp. 338–345, Dec. 2001.

[24] S. Jezernik, R. Wassink, and T. Keller, "Sliding mode closed loop control of FES: Controlling the shank movement," *IEEE Trans. Biomed. Eng.*, vol. 51, no. 2, pp. 263–272, Feb. 2004.

[25] H. Gollee, K. J. Hunt, and D. E. Wood, "New results in feedback control of unsupported standing in paraplegia," *IEEE Trans. Neural Syst. Rehabil. Eng.*, vol. 12, no. 1, pp. 73–80, Mar. 2004.

[26] P. C. Eser, N. d. N. Donaldson, H. Knecht, and E. Stussi, "Influence of different stimulation frequencies on power output and fatigue during FES-cycling in recently injured SCI people," *IEEE Trans. Neural Syst. Rehabil. Eng.*, vol. 11, no. 3, pp. 236–240, Sep. 2003.

[27] H. J. Chizeck, N. Lan, L. S. Palmieri, and P. E. Crago, "Feedback control of electrically stimulated muscle using simultaneous pulsewidth and stimulus period modulation," *IEEE Trans. Biomed. Eng.*, vol. 38, no. 12, pp. 1224–1234, Dec. 1991.

[28] A. B. Z. Karu and W. Durfee, "Reducing muscle fatigue in FES applications by stimulating with n-let pulse trains," *IEEE Trans. Biomed. Eng.*, vol. 42, no. 8, pp. 809–817, Aug. 1995.

[29] P. Mela, P. H. Veltink, P. A. Huijing, S. Salmons, and J. C. Jarvis, "The optimal stimulation pattern for skeletal muscle is dependent on muscle length," *IEEE Trans. Neural Syst. Rehabil. Eng.*, vol. 10, no. 2, pp. 85–92, Jun. 2002.

[30] W. K. Durfee and K. I. Palmer, "Estimation of force-activation, force-length and force-velocity properties in isolated, electrically stimulated muscle," *IEEE Trans. Biomed. Eng.*, vol. 41, no. 3, pp. 205–216, Mar. 1994.

[31] W. K. Durfee, "Task-based methods for evaluating electrically stimulated antagonist muscle pairs," *IEEE Trans. Biomed. Eng.*, vol. 36, no. 3, pp. 309–321, Mar. 1989.

[32] N. Lan, P. E. Crago, and H. J. Chizeck, "Feedback control methods for task regulation by electrical stimulation of muscles," *IEEE Trans. Biomed. Eng.*, vol. 38, no. 12, pp. 1213–1223, Dec. 1991.

[33] A. Ahn, R. Monti, and A. Biewener, "In vivo and *in vitro* heterogeneity of segment length changes in the semimembranosus muscle of the toad," *J. Physiol.*, vol. 549, pp. 877–888, 2003.

[34] J. M. Olson and R. L. Marsh, "Activation patterns and length changes in hindlimb muscles of the bullfrog rana catesbeiana during jumping," *J. Exp. Biol.*, vol. 201, pp. 2763–2777, 1998.

[35] S. J. Schroeck, W. C. Messner, and R. J. McNab, "On compensator design for linear time-invariant dual-input single-output systems," *IEEE/ASME Trans. Mechatronics*, vol. 6, no. 1, pp. 50–57, Mar. 2001.

[36] L. Bernotas, P. E. Crago, and H. J. Chizeck, "A discrete-time model of electrically stimulated muscle," *IEEE Trans. Biomed. Eng.*, vol. BME-33, no. 9, pp. 829–838, Sep. 1986.

[37] N. Hogan, "Adaptive control of mechanical impedance by coactivation of agonist muscles," *IEEE Trans. Autom. Control*, vol. AC-29, no. 8, pp. 681–690, Aug. 1984.

[38] E. Luiker and E. D. Stevens, "Effect of stimulus train duration and cycle frequency on the capacity to do work in the pectoral fin of muscle of the pumpkinseed sunfish, Lopomis gibbosus," *Can. J. of Zool.*, vol. 71, pp. 2185–2189, 1993.

[39] E. D. S. D. Zyme, "Effect of cycle frequency and excursion amplitude on work done by rat diaphragm muscle," *Can. J. Zool.*, vol. 67, pp. 1294–1299, 1989.

[40] E. D. S. J. Renaud, "A comparison between field habits and contractile performance of frog and toad sartorius muscle," *J. Comput. Physiol.*, vol. 151, pp. 127–131, 1983.

[41] A. Ahn and R. Full, "A motor and a brake: Two leg extensor muscles acting at the same joint manage energy differently in a running insect," *J. Exp. Biol.*, vol. 205, pp. 379–389, 2002.

Waleed Farahat received the B.Sc. degree from The American University in Cairo, Cairo, Egypt, in 1997, the S.M. degree, in 2000, from the Massachusetts Institute of Technology, Cambridge, where he is currently working toward the Ph.D. degree in mechanical engineering.

His current research interests include the application of dynamical systems, control, and optimization theories to neuromuscular control, rehabilitation, and robotics.

Hugh Herr received the B.A. degree in physics from Millersville University, Millersville, PA, in 1990, the M.S. degree in mechanical engineering from the Massachusetts Institute of Technology (MIT), Cambridge, and the Ph.D. degree in biophysics from Harvard University, Cambridge, MA, in 1998.

He is Assistant Professor of the Media Laboratory, the Massachusetts Institute of Technology (MIT), Cambridge, and the MIT–Harvard Division of Health Sciences and Technology, Cambridge. His primary research objective is to apply principles of muscle mechanics, neural control, and human biomechanics to guide the designs of biomimetic robots, human rehabilitation devices, and augmentation technologies that amplify the endurance and strength of humans. He has advanced novel actuation strategies, including the use of animal-derived muscle to power robots in the millimeter to centimeter size scale. In the field of human rehabilitation, his group has developed gait adaptive knee prostheses for transfemoral amputees and variable impedance ankle-foot orthoses for patients suffering from drop foot, a gait pathology caused by stroke, cerebral palsy, and multiple sclerosis.